

Stress Analysis of the Lifting Fixture Used in the 2008 Conformal Sonar Array Trials at Seneca Lake

Paul V. Cavallaro
Matthew E. Johnson
Donald L. Cox
Julie C. White
Peter H. Hulton
NUWC Division Newport

Emilio Recine
EG&G Technical Services Inc.



20081014108

**Naval Undersea Warfare Center
Newport, Rhode Island**

PREFACE

This study was funded under job order T141148 by NUWC Division Newport's Hull Arrays and Distributed Sensors Engineering Branch (Code 1514). The principal investigator was Paul V. Cavallaro (Code 70T).

The technical reviewer for this report was Jason M. Maguire (Code 1512).

Reviewed and Approved: 1 September 2008

Harriet L. Coleman

**Harriet L. Coleman
Head, Ranges, Engineering, and Analysis Department**



REPORT DOCUMENTATION PAGE

Form Approved

OMB No. 0704-0188

The public reporting burden for this collection of information is estimated to average 1 hour per response, including the time for reviewing instructions, searching existing data sources, gathering and maintaining the data needed, and completing and reviewing the collection of information. Send comments regarding this burden estimate or any other aspect of this collection of information, including suggestions for reducing this burden, to Department of Defense, Washington Headquarters Services, Directorate for Information Operations and Reports (0704-0188), 1215 Jefferson Davis Highway, Suite 1204, Arlington, VA 22202-4302. Respondents should be aware that notwithstanding any other provision of law, no person shall be subject to any penalty for failing to comply with a collection of information if it does not display a currently valid OPM control number.

PLEASE DO NOT RETURN YOUR FORM TO THE ABOVE ADDRESS.

1. REPORT DATE (DD-MM-YYYY) 01-09-2008		2. REPORT TYPE Final		3. DATES COVERED (From - To)	
4. TITLE AND SUBTITLE Stress Analysis of the Lifting Fixture Used in the 2008 Conformal Sonar Array Trials at Seneca Lake				5a. CONTRACT NUMBER	
				5b. GRANT NUMBER	
				5c. PROGRAM ELEMENT NUMBER	
6. AUTHOR(S) Paul V. Cavallaro, Matthew E. Johnson, Donald L. Cox, Julie C. White, Peter H. Hulton, and Emilio Recine				5.d PROJECT NUMBER	
				5e. TASK NUMBER	
				5f. WORK UNIT NUMBER	
7. PERFORMING ORGANIZATION NAME(S) AND ADDRESS(ES) Naval Undersea Warfare Center Division 1176 Howell Street Newport, RI 02841-1708				8. PERFORMING ORGANIZATION REPORT NUMBER TR 11,882	
9. SPONSORING/MONITORING AGENCY NAME(S) AND ADDRESS(ES)				10. SPONSORING/MONITOR'S ACRONYM	
				11. SPONSORING/MONITORING REPORT NUMBER	
12. DISTRIBUTION/AVAILABILITY STATEMENT Approved for public release; distribution is unlimited.					
13. SUPPLEMENTARY NOTES					
14. ABSTRACT Detailed stress analyses were required of critical lifting fixture components used to support conformal sonar array assemblies in performance trials conducted in 2008 at the Naval Undersea Warfare Center's Seneca Lake Test Facility. The stress analyses were necessary to ensure that the lifting fixture had sufficient structural integrity for the handling and operational phases of the trials. The targeted structural integrity levels required compliance with a minimum safety factor for each of the specific components investigated. The minimum safety factor was set to 5.0 based on the yield stress of each component. The stress analyses examined key screwed connections and weldments that join the lifting fixture to the array modules. The safety factors for the current component designs were determined and compared to the minimum requirement.					
15. SUBJECT TERMS Structural Engineering Stress Analyses Welded Structures Finite Element Modeling Acoustic Arrays					
16. SECURITY CLASSIFICATION OF:			17. LIMITATION OF ABSTRACT SAR	18. NUMBER OF PAGES 29	19a. NAME OF RESPONSIBLE PERSON Paul V. Cavallaro
a. REPORT Unclassified	b. ABSTRACT Unclassified	c. THIS PAGE Unclassified			19b. TELEPHONE NUMBER (Include area code) 401-832-5082

TABLE OF CONTENTS

Section	Page
LIST OF ILLUSTRATIONS.....	ii
LIST OF TABLES.....	ii
LIST OF ABBREVIATIONS, ACRONYMS, AND SYMBOLS	iii
1 INTRODUCTION	1
1.1 Purpose.....	1
1.2 Background.....	1
1.3 Approach.....	3
2 MODEL DEVELOPMENT	5
3 STRESS ANALYSIS.....	7
3.1 Determination of Stress Resultants.....	7
3.2 Stress Analysis of I-Beam-to-Adapter-Plate Welds	8
3.3 Stress Analysis of Standoff Pipes	11
3.4 Stress Analysis of the I-Beam-to-Adapter-Plate Screws	12
3 SUMMARY AND CONCLUSIONS	21
REFERENCES	22

LIST OF ILLUSTRATIONS

Figure	Page
1 Configuration 1 Test Fixture Assembly.....	2
2 Geometric Properties of a Wide-Flange (W10 x 60) Steel I-Beam.	2
3 Locations of I-Beam-to-Adapter-Plate Fillet Welds.....	2
4 Finite Element Model of Test Fixture/Array Panels Assembly Used to Obtain Stress Resultants at Connection Points.	5
5 ABAQUS Model of Configuration 1 Assembly Showing the 1-g Deadweight and Overturning Load Cases.....	6
6 ABAQUS Model of Configuration 2 Assembly Showing the 1-g Deadweight and Overturning Load Cases.....	6
7 Definition of Weld Throat for the Fillet-Welded I-Beam-to-Adapter-Plate Connection.	9
8 Centroid Location of Adapter Plate Screw Group Pattern.....	13
9 Eccentric Shear Loading Path for Adapter-Plate-to-Array Screws.	15

LIST OF TABLES

Table	Page
1 Configuration 1 Array/Test Fixture Assembly Description and Component Weights.....	3
2 Stress Resultants at Connection Points for the Configuration 1 Assembly Deadweight Load Case.	7
3 Stress Resultants at Connection Points for the Configuration 2 Assembly Deadweight Load Case.	7
4 Stress Resultants at Connection Points for the Configuration 1 Assembly Overturning Plus 1-g Vertical Load Case.	8
5 Stress Resultants at Connection Points for the Configuration 2 Assembly Overturning Plus 1-g Vertical Load Case.	8
6 Yield and Allowable Stress Values.....	11
7 Mechanical Properties of ASTM A325 1.25-In.-Diameter Steel Screws.....	12
8 Maximum Moments at the Adapter-Plate-to-Array-Plate Joints.	12
9 Screw Axial Reaction Forces Resulting from Bending Moment M_x	14
10 Resultant Joint and Primary Screw Shearing Forces and Averaged Screw Shear Stresses.....	16
11 Bending Stresses Due to Load Path Eccentricity.....	17
12 Total Screw Axial Forces.....	18
13 Total Screw Normal Stresses.	19
14 Maximum Screw Principal Stresses.....	19
15 Safety Factors on Screw Principal Stresses.	20
16 Average Screw Thread Shear Stresses and Safety Factors.....	20

LIST OF ABBREVIATIONS, ACRONYMS, AND SYMBOLS

A_{nom}	Cross sectional area of screw based on nominal diameter
A_s	Shear area of screw
ASTM	American Society for Testing Materials
A_t	Tensile area of screw
A_w	Total throat area of fillet weld
b	Width of I-beam flanges
DOF	Degrees of freedom
d	Distance between I-beam outer flange surfaces
d_{inner}	Inner diameter of standoff pipes
d_{nom}	Nominal diameter of screw
d_{outer}	Outer diameter of standoff pipes
d_s	Shear diameter of screw
d_t	Tensile diameter of screw
D_{flats}	Distance between flat regions of screw head
E_{plates}	Elastic modulus of plates
E_{screw}	Elastic modulus of screw
$F_{dp1}, F_{dp2}, F_{dp3}$	Axial reaction forces for screw rows 1, 2, and 3
$F_{joint\ shear}$	Total shear force on adapter-plate-to-array-plate joint
$F_{preload}$	Screw preload force
$F_{shear\ screw}$	Total shear force on screws in adapter-plate-to-array-plate joint
F_{screw_total}	Total axial force in screw
F_x, F_y, F_z	Forces aligned in x-, y-, and z-directions
g	Acceleration due to gravity ($1\ g = 386.4\ \text{in./s}^2$)
h	Leg dimension of fillet weld
ID	Inside diameter
I_{u_x}, I_{u_y}	Unit moments of inertia of welds about x- and y-directions
I_{tot_x}, I_{tot_y}	Total moments of inertia of welds about x- and y-directions
$k_{adapter\ plate}$	Compressive stiffness of adapter plate
k_{array}	Compressive stiffness of array plate
k_{joint}	Compressive stiffness of joint members
k_{screw}	Axial stiffness of screw
L_{arm}	Length of moment arm in screw
L_{grip}	Effective grip length of screw
L_w	Total length of fillet weld
K	Torque coefficient
M_x, M_y, M_z	Moments aligned in x-, y-, and z-directions
NSRF	Normal stress reduction factor of fillet weld
OD	Outside diameter
$r1, r2, r3$	Distance from screw group centroid to screw rows 1, 2, and 3
SF	Safety factor
$SF_{pipebend}$	Safety factor on standoff pipe bending stress
SF_{prin_weld}	Safety factor on principal stress of fillet weld
$SF_{shearstressweld}$	Safety factor on shear stress of fillet weld

LIST OF ABBREVIATIONS, ACRONYMS, AND SYMBOLS (Cont'd)

$SSRF$	Shear stress reduction factor of fillet weld
σ_{AS}	Allowable shear stress in fillet weld
σ_{bend_ecc}	Bending stress in screw due to load path eccentricity
$\sigma_{max\ prin}$	Maximum principal stress in screw
σ_{NS}	Allowable normal stress in fillet weld
$\sigma_{pipebend}$	Bending stress in standoff pipes
σ_{prin_weld}	Maximum principal stress in fillet weld
σ_{sy_plate}	Shear yield stress of array plate
σ_{total}	Total normal stress in screw
σ_{total_weld}	Total normal stress in fillet weld
σ_y_I-beam	Tensile yield stress of I-beam
σ_y_pipe	Tensile yield stress of standoff pipe
σ_y_plate	Tensile yield stress of array plate
σ_y_screw	Tensile yield stress of screw
T	Screw torque
$t_{adapter\ plate}$	Thickness of adapter plate
$t_{array\ plate}$	Thickness of array plate
t_f	Thickness of I-beam flanges
t_w	Thickness of I-beam web
τ_{screw}	Average shear stress in screw
$\tau_{threads}$	Average shear pull-out stress in plate threads
τ_{weld}	Shear stress in fillet weld
Y	Distance from reference axis to screw

STRESS ANALYSIS OF THE LIFTING FIXTURE USED IN THE 2008 CONFORMAL SONAR ARRAY TRIALS AT SENECA LAKE

1. INTRODUCTION

1.1 PURPOSE

Detailed stress analyses were required of critical lifting fixture components used to support conformal sonar array assemblies in performance trials conducted in 2008 at the Naval Undersea Warfare Center's Seneca Lake Test Facility. The stress analyses were necessary to ensure that the test fixture had sufficient structural integrity for the handling and operational phases of the trials. The targeted structural integrity levels had to be in compliance with a minimum safety factor for each of the components. The minimum safety factor was set to 5.0 based on the yield stress of each component.

The stress analyses documented in this report examined key screwed connections and weldments that join the lifting fixture to the array panels. The safety factors for the current component designs were determined and compared to the minimum requirement.

1.2 BACKGROUND

The steel lifting fixture assembly, illustrated in figure 1, was designed to mount two test panels back-to-back to reduce test time at Seneca Lake. The main load-carrying element of the fixture is an I-beam with a central lifting plate attached at its mid-span. The I-beam (see figure 2 for cross-sectional illustration) supports two array panels, one panel located at each end. An adapter plate, which is welded to each end of the I-beam using fillet welds (see figure 3), facilitates connection of the test panels to the I-beam. Mechanical fasteners were used to join the adapter plates to the array panels for assembly/disassembly purposes.

Figure 1 provides a cursory description of the weldments and fastener arrangements. (Each array assembly includes a proportionately sized backplate, test panel, and one pair of vibration shakers.) Four horizontal standoff pipes having an outsider diameter of 3.5 in. and an inside diameter of 2.9 in. are welded in place between opposing corners of the array assemblies to produce a box-like reinforcement.

During the trials, two configurations—referred to as Configuration 1 and Configuration 2—will be evaluated by changing the test panels attached to the lifting fixture. Component weights (in air) and piece-part counts are provided in table 1 for the Configuration 1 test. While the weight breakdown of the Configuration 2 test is not available, the total suspended weight has been given as 15,894 pounds. During the Configuration 2 test, the lifting fixture/array assembly is configured with up to 1000 pounds of counterweight as required for balancing purposes.

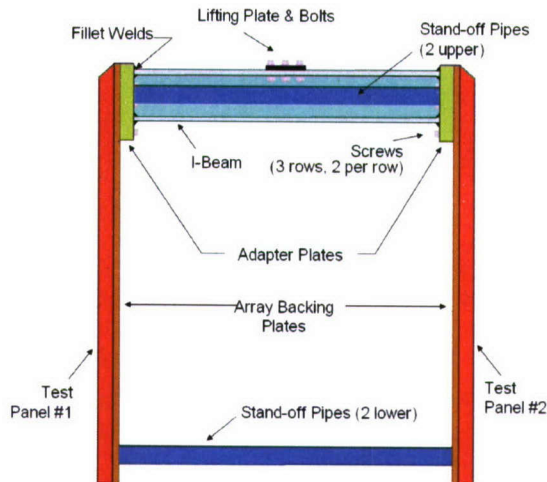
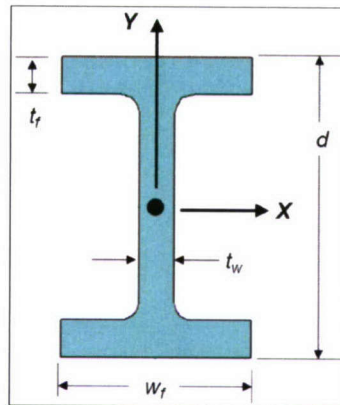


Figure 1. Configuration 1 Test Fixture Assembly



Nominal Size (in x lb/ft)	Cross Sectional Area (in ²)	Depth <i>d</i> (in)	Flange Width <i>w_f</i> (in)	Flange Thick. <i>t_f</i> (in)	Web Thick. <i>t_w</i> (in)	Moment of Inertia <i>I_{xx}</i> (in ⁴)	Moment of Inertia <i>I_{yy}</i> (in ⁴)	Section Modulus <i>Z_{xx}</i> (in ³)	Section Modulus <i>Z_{yy}</i> (in ³)	Radius of Gyration <i>K_{xx}</i> (in)	Radius of Gyration <i>K_{yy}</i> (in)
W10 X 60	17.60	10.22	10.08	0.68	0.42	341.00	116.00	66.70	23.00	4.39	2.57

Figure 2. Geometric Properties of a Wide-Flange (W10 x 60) Steel I-Beam

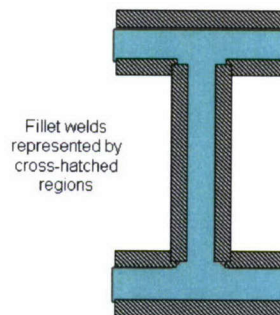


Figure 3. Locations of I-Beam-to-Adapter-Plate Fillet Welds

Table 1. Configuration 1 Array/Test Fixture Assembly Description and Component Weights

Item Description	Unit Weight (lb)	Quantity	Total Weight (lb)
I-Beam (steel, 10 x 10 x 60 in. WF 65 lb/ft)	325.0	1	325.0
Junction Boxes	100.0	2	200.0
Steel Plate (92 x 110 x 1 in.)	2,874.0	2	5,748.0
Acoustic Array	2,538.0	2	5,076.0
Vibration Shaker	100.0	4	400.0
Balance Weight	1,000.0	1	1,000.0
Pipes (steel, 3.5-in. OD x 2.9-in. ID)	51.4	4	205.6
Grand Total Weight			12,954.6

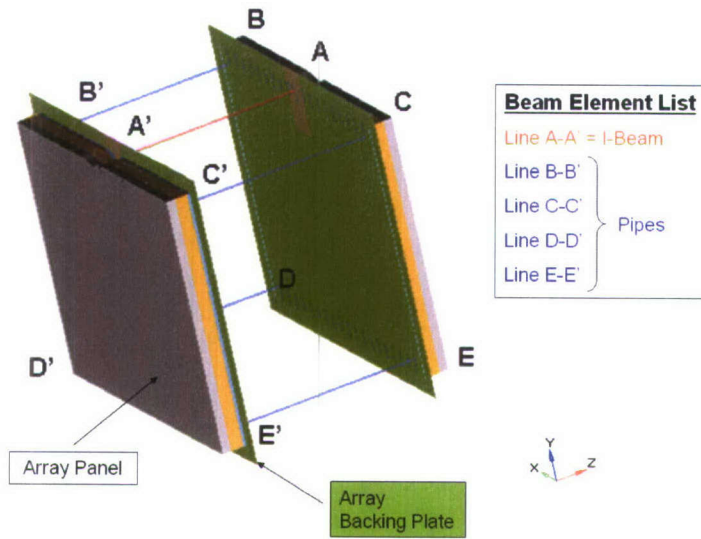
The test fixture is designed to vertically suspend the array assemblies during transport (via a crane system) between a pre-designated pierside location and a floating barge, as well as during submerged acoustic testing. When the barge reaches its destination point, the fixture/array assemblies will be lowered into the lake and acoustic testing will commence. Upon completion of the acoustic tests, the process will be reversed to return the array assemblies to the pier.

1.3 APPROACH

Stress analysis of the screwed and welded regions required the determination of stress resultants (reaction forces and moments) at each connection point. Global finite element models of the two configurations were generated using ABAQUS analysis software¹ to provide static solutions of stress resultants (rather than actual stresses) at each connection (node) corresponding to two load cases. Stress resultants obtained from each load case were then used in closed-form solutions to calculate stresses in the individual welds and screws. Comparisons of these stresses to the yield stresses of the appropriate component provided the safety factors for the respective components.

2. MODEL DEVELOPMENT

The finite element model of the lifting fixture and array assemblies was generated using a variety of element types (see figure 4). The array panels were represented using 3-D continuum (solid) elements; the array backing plates and adapter plates were modeled using shell elements; and the I-beam and standoff pipes were modeled using 3-D beam elements.



Note: The coordinate system defines the local orientation axes of the I-beam and standoff pipe beam elements.

**Figure 4. Finite Element Model of Test Fixture/Array Panels Assembly
Used to Obtain Stress Resultants at Connection Points**

Force and moment reactions were sought at critical connection points for two load cases. The first load case was a 1-g vertical (deadweight) suspension as shown on the left side of figures 5 and 6. Deadweight loading was performed using a body force acceleration of 386.4 in./s^2 (1 g) applied along the vertical (upward, +Y) direction. Displacement boundary conditions consisted of fixing the translational and rotational degrees of freedom (DOFs) at the I-beam mid-span node to simulate the crane's cable suspension point. The second load case, shown on the right side of figures 5 and 6, was established for conservative design purposes to provide the fixture with sufficient structural integrity should excessive or improper handling occur. This case combined the 1-g vertical deadweight load with an overturning event. The overturning event applied a push force with the vector aligned in the Z-axis passing through the centroid of the I-beam. For the overturning load case, the 1-g vertical body force acceleration was applied to simulate deadweight along with an enforced 3-in. displacement in the -Z-direction applied above connection point A so that the edge defined below connection points D and E experienced vertical lift-off. All loads were assumed to be statically applied, and material properties were treated as linearly elastic. Checks were performed to ensure that the sum of all forces and moments was exactly zero—as required for static equilibrium. The obtained stress resultants were then used in closed-form solutions of the individual weld and screw stresses.

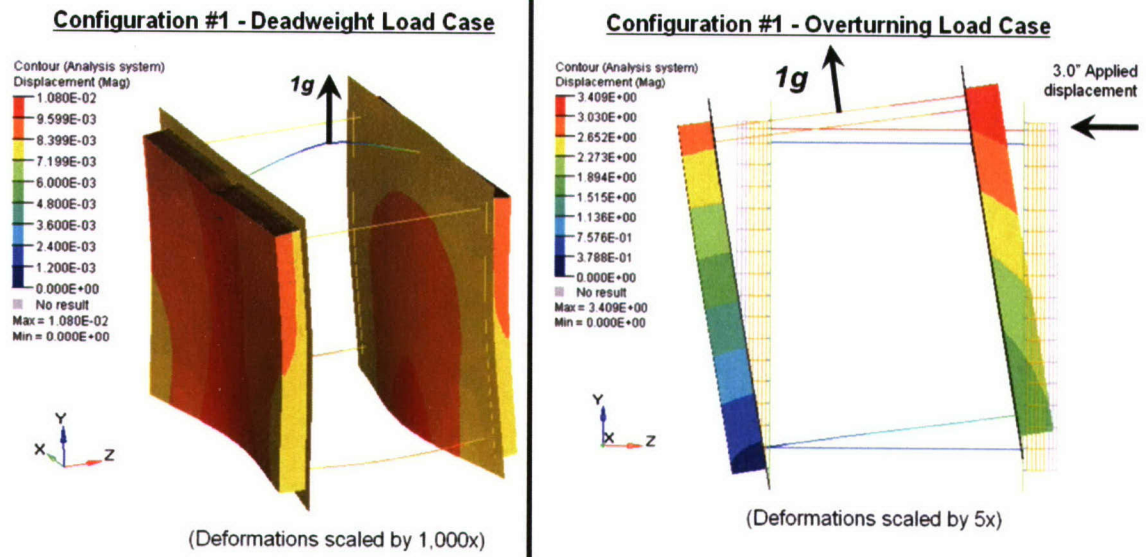


Figure 5. ABAQUS Model of Configuration 1 Assembly Showing the 1-g Deadweight and Overturning Load Cases (Contours represent resultant displacement magnitudes.)

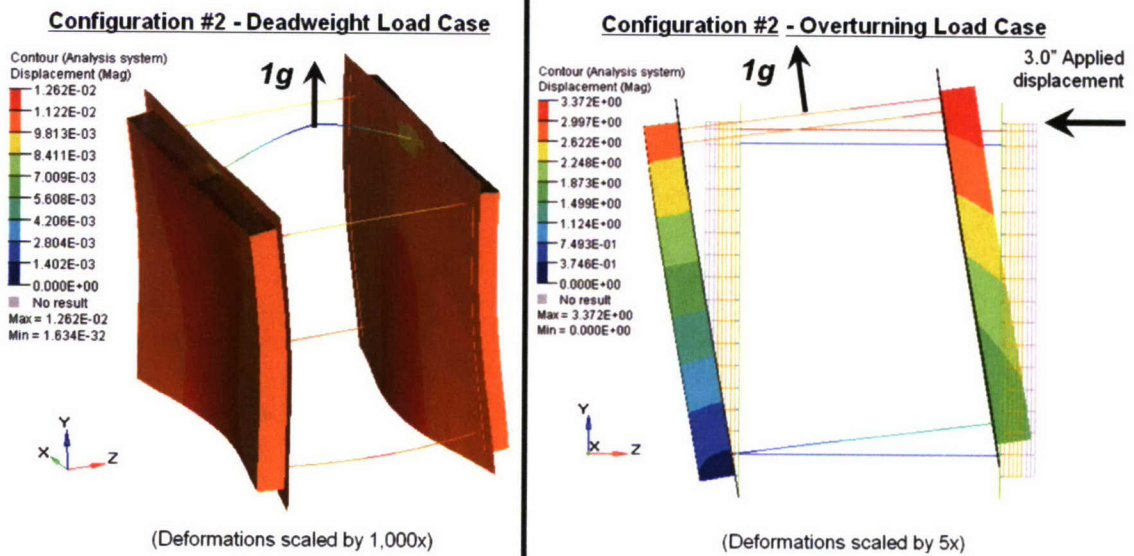


Figure 6. ABAQUS Model of Configuration 2 Assembly Showing the 1-g Deadweight and Overturning Load Cases (Contours represent resultant displacement magnitudes.)

3. STRESS ANALYSIS

3.1 DETERMINATION OF STRESS RESULTANTS

Tables 2 through 5 list the stress resultants (forces and moments) acting at each connection point for Configurations 1 and 2 subjected to the deadweight and overturning load cases. Note that F_X and F_Y represent orthogonal shearing forces, F_Z represents axial force, moments M_X and M_Y represent bending moments, and M_Z represents torque.

Table 2. Stress Resultants at Connection Points for the Configuration 1 Assembly Deadweight Load Case

Location	F_x (lb)	F_y (lb)	F_z (lb)	M_x (in.-lb)	M_y (in.-lb)	M_z (in.-lb)
A	141.20	-6,347.00	0.00	-15,322.00	0.00	0.00
A'	141.20	6,347.00	0.00	-15,322.00	0.00	0.00
B	19.25	23.04	0.00	-315.50	-63.63	0.00
B'	19.25	-23.04	0.00	-315.50	-63.63	0.00
C	19.25	23.04	0.00	-315.50	63.63	0.00
C'	19.25	-23.04	0.00	-315.50	63.63	0.00
D	-89.87	23.04	0.00	-7.41	-453.70	0.00
D'	-89.87	-23.04	0.00	-7.41	-453.70	0.00
E	-89.87	23.04	0.00	-7.41	453.70	0.00
E'	-89.87	-23.04	0.00	-7.41	453.70	0.00

Table 3. Stress Resultants at Connection Points for the Configuration 2 Assembly Deadweight Load Case

Location	F_x (lb)	F_y (lb)	F_z (lb)	M_x (in.-lb)	M_y (in.-lb)	M_z (in.-lb)
A	162.90	-7,947.00	0.00	-19,089.00	0.00	0.00
A'	162.90	7,947.00	0.00	-19,089.00	0.00	0.00
B	14.87	23.04	0.00	-369.20	-85.39	0.00
B'	14.87	-23.04	0.00	-369.20	-85.39	0.00
C	14.87	23.04	0.00	-369.20	85.39	0.00
C'	14.87	-23.04	0.00	-369.20	85.39	0.00
D	-96.34	23.04	0.00	29.20	-492.20	0.00
D'	-96.34	-23.04	0.00	29.20	-492.20	0.00
E	-96.34	23.04	0.00	29.20	492.20	0.00
E'	-96.34	-23.04	0.00	29.20	492.20	0.00

Table 4. Stress Resultants at Connection Points for the Configuration 1 Assembly Overturning Plus 1-g Vertical Load Case

Location	F_x (lb)	F_y (lb)	F_z (lb)	M_x (in.-lb)	M_y (in.-lb)	M_z (in.-lb)
A	-2,098.00	-3,226.00	0.00	108,780.00	0.00	0.00
A'	-2,098.00	-3,700.00	0.00	-78,223.00	0.00	0.00
B	154.80	-474.30	-90.11	14,097.00	-2,466.00	-3.47
B'	154.80	-520.40	-90.11	-12,762.00	2,400.00	-3.47
C	154.80	-474.30	90.11	14,097.00	2,466.00	3.47
C'	154.80	-520.40	90.11	-12,762.00	-2,400.00	3.47
D	-1,252.00	-1,040.00	-156.60	25,120.00	-5,783.00	1.80
D'	-1,252.00	-1,086.00	-156.60	-32,280.00	2,675.00	1.80
E	-1,252.00	-1,040.00	156.60	25,120.00	5,783.00	-1.80
E'	-1,252.00	-1,086.00	156.60	-32,280.00	-2,675.00	-1.80

Table 5. Stress Resultants at Connection Points for the Configuration 2 Assembly Overturning Plus 1-g Vertical Load Case

Location	F_x (lb)	F_y (lb)	F_z (lb)	M_x (in.-lb)	M_y (in.-lb)	M_z (in.-lb)
A	-2,623.00	-4,069.00	0.00	135,160.00	0.00	0.00
A'	-2,623.00	-4,543.00	0.00	-97,353.00	0.00	0.00
B	184.10	-595.30	-111.70	17,548.00	-3,065.00	-4.32
B'	184.10	-641.40	-111.70	-15,842.00	2,969.00	-4.32
C	184.10	-595.30	111.70	17,548.00	3,065.00	4.32
C'	184.10	-641.40	111.70	-15,842.00	-2,969.00	4.32
D	-1,541.00	-1,298.00	-193.00	31,262.00	-7,105.00	2.21
D'	-1,541.00	-1,344.00	-193.00	-40,077.00	3,315.00	2.21
E	-1,541.00	-1,298.00	193.00	31,262.00	7,105.00	-2.21
E'	-1,541.00	-1,344.00	193.00	-40,077.00	-3,315.00	-2.21

3.2 STRESS ANALYSIS OF I-BEAM-TO-ADAPTER-PLATE WELDS

The adapter plates are connected to each end of the I-beam using fillet welds along the full perimeter of the I-beam cross section. In accordance with Shigley and Mischke,² the unit moments of inertia I_{u_x} , and I_{u_y} for the I-beam-to-adapter-plate welds are approximated by

$$I_{u-X} = \frac{(d - 2t_f)^3}{6} + \frac{(b - t_w)(d - 2t_f)^2}{2} + \frac{bd^2}{2} = 1,023.63 \text{ in.}^3, \quad (1)$$

$$I_{u-Y} = \frac{b^3}{6} + \frac{(b - t_w)^3}{6} + \frac{(d - 2t_f)t_w^2}{2} = 321.72 \text{ in.}^3, \quad (2)$$

where d is the vertical distance between flange outer edges, t_f is the flange thickness, b is the flange width, and t_w is the web thickness.

The total moments of inertia for the fillet weld with leg dimension h equal to 0.4 in. are given by

$$I_{tot-X} = \frac{\sqrt{2}}{2} h I_{u-X} = 289.24 \text{ in.}^4, \quad (3)$$

$$I_{tot-Y} = \frac{\sqrt{2}}{2} h I_{u-Y} = 91.00 \text{ in.}^4, \quad (4)$$

where $\frac{\sqrt{2}}{2} h$ is referred to as the weld throat dimension as shown in figure 7.

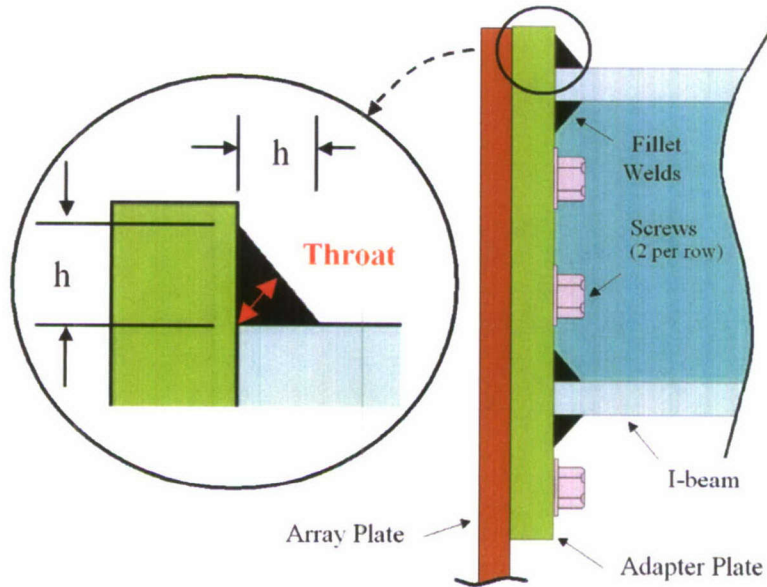


Figure 7. Definition of Weld Throat for the Fillet-Welded I-Beam-To-Adapter-Plate Connection (Arrays and standoff pipes not shown.)

Summing the length of each weld, one obtains the total weld length L_w :

$$L_w = 2b + 2(d - 2t_f) + 2(b - t_w) = 56.69 \text{ in.} \quad (5)$$

Therefore, the total weld area A_w is computed by

$$A_w = \frac{\sqrt{2}}{2} h L_w = 16.18 \text{ in.}^2. \quad (6)$$

The total normal stress σ_{tot} acting on the weld is obtained through superposition of the sum of the axial and bending stress components:

$$\sigma_{total_weld} = \frac{F_{ZA}}{A_w} + \frac{M_{XA} \frac{d}{2}}{I_{tot_X}} + \frac{M_{YA} \frac{b}{2}}{I_{tot_Y}}. \quad (7)$$

	Total Normal Stress in Weld (psi)	
Load Case	Configuration 1	Configuration 2
Deadweight	270.69	337.25
Overturning	1,921.82	2,387.87

The average shear stress in the weld τ_w is computed by

$$\tau_{weld} = \frac{\sqrt{F_{XA'}^2 + F_{YA'}^2}}{A_w}. \quad (8)$$

	Average Shear Stress in Weld (psi)	
Load Case	Configuration 1	Configuration 2
Deadweight	395.94	495.73
Overturning	265.27	327.16

The maximum principal stress in the weld σ_{prin_weld} is obtained by

$$\sigma_{prin_weld} = \frac{\sigma_{total_weld}}{2} + \sqrt{\left(\frac{\sigma_{total_weld}}{2}\right)^2 + \tau_{weld}^2} \quad (9)$$

	Max. Principal Stress in Weld (psi)	
Load Case	Configuration 1	Configuration 2
Deadweight	553.78	692.24
Overturning	1,957.76	2,431.88

Table 6 lists the tensile yield stress for the I-beam and the allowable normal and shear stresses for the welds. Note that each weld is assumed to be perfect (that is, free of inclusions, cracks, etc.) and to be fully capable of developing the allowable stress values shown.

Table 6. Yield and Allowable Stress Values

I-Beam Tensile Yield Stress ($\sigma_{y \text{ I-beam}}$) (psi)	36,000
Normal Stress Reduction Factor (NSRF)	0.40
Allowable Normal Stress in Weld (σ_{AN}) (psi)	14,400
Shear Stress Reduction Factor (SSRF)	0.40
Allowable Shear Stress in Weld (σ_{AS}) (psi)	5,760

The normal and shear stress reduction factors for the weld material, NSRF and SSRF, respectively, were applied to obtain the “as-welded” allowable strengths of the weld metal and were based on the American Institute of Steel Construction’s code for building construction as shown in Shigley and Mischke.² Note that the weld allowable shear stress σ_{AS} was computed by applying SSRF to the allowable normal stress σ_{AN} . The resulting safety factors for the principal and shear weld stresses are

$$SF_{\text{prin_weld}} = \frac{\sigma_{AN}}{\sigma_{\text{prin_weld}}},$$

	Safety Factor on Principal Stress	
Load Case	Configuration 1	Configuration 2
Deadweight	26.00	20.80
Overturning	7.36	5.92

(10)

and

$$SF_{\text{shearstressweld}} = \frac{\sigma_{AS}}{\tau_{\text{weld}}}.$$

	Safety Factor on Shear Stress	
Load Case	Configuration 1	Configuration 2
Deadweight	14.550	11.62
Overturning	21.71	17.61

(11)

3.3 STRESS ANALYSIS OF STANDOFF PIPES

The maximum bending stress within the standoff pipes is computed by

$$\sigma_{\text{pipebend}} = \frac{\sqrt{M_{XB}^2 + M_{YB}^2} \left(\frac{d_{\text{outer}}}{2} \right)}{\pi \left(\frac{d_{\text{outer}}^4 - d_{\text{inner}}^4}{64} \right)}.$$

	Max. Bending Stress in Standoff Pipes	
Load Case	Configuration 1	Configuration 2
Deadweight	203.91	221.57
Overturning	14,555.47	18,071.011

(12)

The tensile yield stress of the standoff pipes $\sigma_{y \text{ pipe}}$ is 36,000 psi. Therefore, the safety factor on pipe bending is

$$SF_{pipebend} = \frac{\sigma_{y_pipe}}{\sigma_{pipebend}}.$$

Load Case	Safety Factor in Standoff Pipes	
	Configuration 1	Configuration 2
Deadweight	176.55	162.48
Overturning	2.47	1.99

(13)

3.4 STRESS ANALYSIS OF I-BEAM-TO-ADAPTER-PLATE SCREWS

A stress analysis was performed to establish the available safety factors for each screw within the adapter-plate-to-array joints. The joints include six 1.25-in.-nominal-diameter d_{nom} ASTM A325 steel screws torqued to 160 ft-lb. The geometric and strength properties of these screws are shown in table 7. Using the stress resultants obtained from the finite element analyses corresponding to the deadweight and overturning load cases, the maximum moments developed within the adapter-plate-to-array joints were along the X -direction and are listed in table 8.

Table 7. Mechanical Properties of ASTM A325 1.25-In.-Diameter Steel Screws³

Nominal Diameter d_{nom} (in.)	Tensile Diameter d_t (in.)	Shear Diameter d_s (in.)	Nominal Area A_{nom} (in. ²)	Tensile Area A_t (in. ²)	Shear Area A_s (in. ²)	Proof Stress σ_{proof_screw} (ksi)	Yield Stress σ_{y_screw} (ksi)	Tensile Stress $\sigma_{tensile_screw}$ (ksi)
1.25	1.11	1.065	1.227	0.969	0.891	74.00	81.00	105.00

Table 8. Maximum Moments at the Adapter-Plate-To-Array-Plate Joints

Load Case	Maximum Moment M_x (in.-lb) at Adapter Plates	
	Configuration 1	Configuration 2
Deadweight	-15,322	-19,089
Overturning	108,780	135,160

Note that, because of the coordinate system used in figure 4, negative values of M_x exert tension on screws located above the screw group centroid. Conversely, positive values of M_x exert tension on screws located below this centroid. No screw tension results from negative values of

M_x in screws located below the centroid. Similarly, no screw tension develops from positive values of M_x on screws located above the centroid. Load transfer in the vicinity of screws subjected to the latter two conditions is accomplished by the adapter plates pushing on the array plates.

Bending moment M_x acts at the centroid location of the screw group. Figure 8 shows the relative screw positions used to support the calculation of the screw group centroid with respect to a chosen reference axis. This reference axis is the horizontal line passing through the centers of the bottom two screws. The combined centroid location is given as \bar{Y} and is measured from the reference axis according to

$$\bar{Y} = \frac{\sum_{i=1}^6 Y_i A_{ti}}{\sum_{i=1}^6 A_{ti}} = 5.183 \text{ in.}, \quad (14)$$

where Y is the vertical distance from the reference axis to the screw of interest, and A_t is the tensile area of the screw.

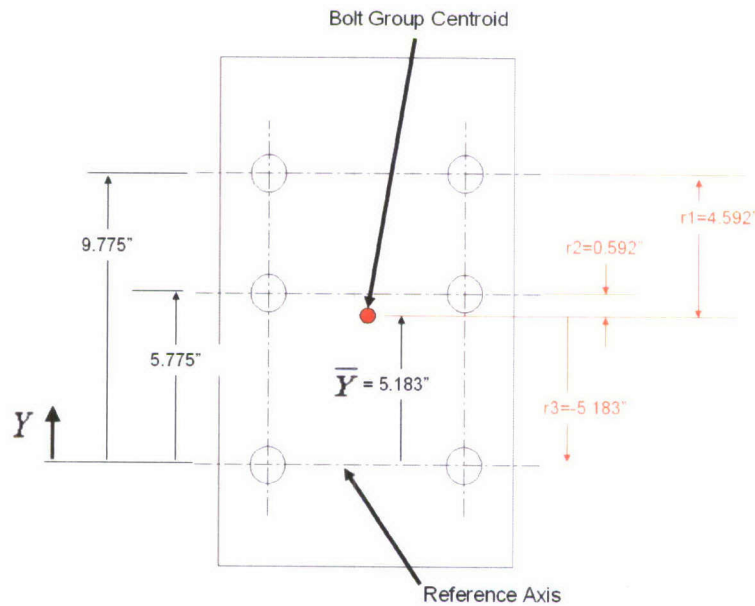


Figure 8. Centroid Location of Adapter Plate Screw Group Pattern

Bending moments developed at the screw group centroid (as reported in tables 2 through 5) are reacted by axial screw forces, designated as F_{dp1} , F_{dp2} , and F_{dp3} in rows 1, 2, and 3, respectively. Because M_y is identically zero at locations A and A' for both the deadweight and overturning load cases, screws of a given row have identical axial reaction forces. By enforcing static equilibrium, the following equation relates the bending moment to the individual screw axial reaction forces:

$$M_x = 2 (F_{dp1}r1 + F_{dp2}r2 + F_{dp3}r3). \quad (15)$$

The factor of 2 in equation (15) is required because two screws are present within each row. Since the screws are of the same material and have equal diameters, the relationship between axial reaction forces among the screws is given by

$$\frac{F_{dp1}}{r1} = \frac{F_{dp2}}{r2} = \frac{F_{dp3}}{r3}. \quad (16)$$

The axial reaction forces, obtained by substituting equation (16) into equation (15), are given by

$$F_{dp1} = \frac{M_x}{2 \left(r1 + \frac{r2^2}{r1} + \frac{r3^2}{r1} \right)},$$

$$F_{dp2} = \frac{M_x}{2 \left(r2 + \frac{r1^2}{r2} + \frac{r3^2}{r2} \right)}, \quad (17)$$

$$F_{dp3} = \frac{M_x}{2 \left(r3 + \frac{r1^2}{r3} + \frac{r2^2}{r3} \right)},$$

where M_x is set to the greater magnitude of bending moments M_{AX} and $M_{AX'}$. The axial reaction forces are given in table 9.

Table 9. Screw Axial Reaction Forces Resulting from Bending Moment M_x

	Deadweight Load Case		Overturning Load Case	
	Configuration 1	Configuration 2	Configuration 1	Configuration 2
Maximum M_x (in.-lb)	-15,322	-19,089	108,780	135,160
Maximum M_x Location	A and A'	A and A'	A	A
Screw Location	Screw Axial Reaction Forces (lb)			
F_{dp1}	-728.29	-907.35	5,170.57	6,424.48
F_{dp2}	-93.85	-116.92	666.26	827.84
F_{dp3}	822.14	1,024.26	-5,836.83	-7,252.31
Note: Negative values indicate tensile axial reactions; positive values indicate joint compression.				

The screw preload force resulting from the 160-ft-lb torque requirement is approximated by equation (18), assuming a torque coefficient of 0.2:

$$F_{preload} = \frac{T}{K d_{nom}} = 7,680 \text{ lb}, \quad (18)$$

where T is the torque, K is the torque coefficient, and d_{nom} is the nominal diameter. Comparing $F_{preload}$ to the tensile axial reaction forces in table 9 indicates that joint separation will not occur because the condition $F_{preload} > F_{dp1}$, F_{dp2} , and F_{dp3} is met.

The adapter-plate-to-I-beam joint develops a load path eccentricity as shown in figure 9. Therefore, localized screw bending stresses are generated in each screw. However, the most difficult aspect of understanding screw bending behavior in eccentrically loaded joints is the determination of the moment arm, as stated by Bruhn.⁴ Therefore and in comparison with Bruhn, a more conservative bending moment arm L_{arm} was assumed as

$$L_{arm} = \frac{t_{adapterplate} + t_{arrayplate}}{2} = 1.375 \text{ in.}, \quad (19)$$

where $t_{adapterplate}$ is the thickness of the adapter plate (= 1.75 in.), and $t_{arrayplate}$ is the thickness of array plate (= 1.00 in.).

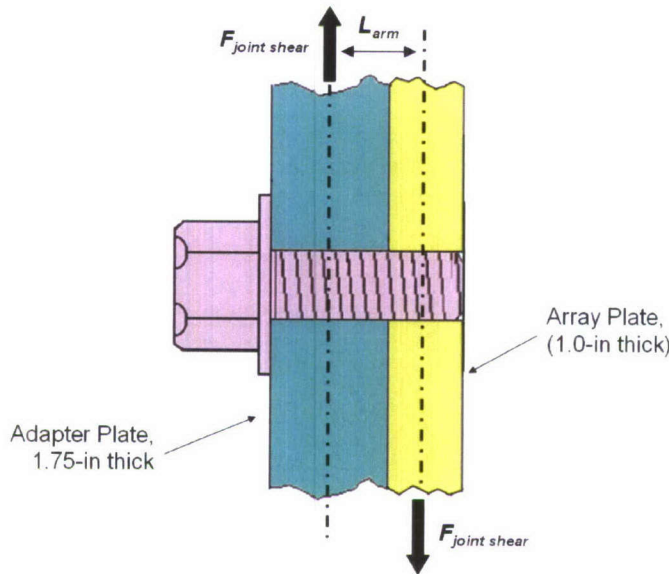


Figure 9. Eccentric Shear Loading Path for Adapter-Plate-to-Array Screws

The total shearing force on the adapter-plate-to-array-plate joint is $F_{joint\ shear}$, as shown in figure 9. This entire shear force is assumed to be uniformly distributed to each screw (i.e., no transfer is assumed through friction between the plates) so that the primary shearing force per screw $F_{shearscrew}$ is given by

$$F_{shearscrew} = \frac{F_{joint\ shear}}{6}, \quad (20)$$

where $F_{joint\ shear}$ is the resultant shearing force computed by

$$F_{joint\ shear} = \sqrt{F_X^2 + F_Y^2}. \quad (21)$$

The averaged shear stress on each screw τ_{screw} is obtained as

$$\tau_{screw} = \frac{F_{shearscrew}}{A_s}, \quad (22)$$

where A_s is the screw shear area ($= 0.890 \text{ in.}^2$). The corresponding values of $F_{joint\ shear}$, $F_{shearscrew}$, and τ_b are specified in table 10.

Table 10. Resultant Joint and Primary Screw Shearing Forces and Averaged Screw Shear Stresses

Maximum Location	Resultant Joint Shear Force (lb)		Primary Screw Shear Force (lb)		Averaged Screw Shear Stress (psi)	
	Configuration 1	Configuration 2	Configuration 1	Configuration 2	Configuration 1	Configuration 2
A and A'	6,349	7,949	1,058	1,325	1,189	1,489
A'	4,253	5,246	709	874	796	982

The maximum screw bending stress due to load path eccentricity occurs on the surface of the screw and is a function of the primary screw shearing force. This bending stress is given by

$$\sigma_{bend_ecc} = \frac{16 F_{shearscrew} L_{arm}}{\pi d_i^3}. \quad (23)$$

The screws behave as cantilevered beams, with one end fixed and the other end guided so that rotation at both ends is restrained. Therefore, equation (23) includes the appropriate reduction factor of $\frac{1}{2}$ applied to the moment. These bending stresses are given in table 11.

Table 11. Bending Stresses Due to Load Path Eccentricity

	Screw Bending Stress Due to Load Path Eccentricity (psi)	
Load Case	Configuration 1	Configuration 2
Deadweight	5,403	6,766
Overturning	3,621	4,463

Next, the screw and joint member stiffnesses (k_{screw} and k_{joint} , respectively) are computed for use in calculating the combined screw stresses due to the axial reaction and preload forces. (Guidance is provided by Shigley and Mischke² on computing k_{joint} for bolted connections (i.e., configured with nuts). However, the joints investigated here utilize threaded holes in the array plates rather than nuts. It has been assumed that Shigley's method for characterizing joint member stiffness is applicable to plates having threaded holes in contrast with joints having bolted connections. Further investigation may be warranted.)

The effective grip length L_{grip} of a screw used with a threaded hole (rather than a nut) is approximated by equation (24) (for the condition $t_{array\ plate} > d_{nom}$):

$$L_{grip} = t_{washer} + t_{adapter_plate} + \frac{d_{nom}}{2} = 2.47 \text{ in.}, \quad (24)$$

where t_{washer} is the washer thickness (= 0.165 in.). The screw stiffness is then conservatively computed according to equation (25):

$$k_{screw} = \frac{A_t E_{screw}}{L_{grip}} = 11.77 \times 10^6 \text{ lb/in.}, \quad (25)$$

where A_t is the screw cross-sectional area based on tensile diameter, and E_{screw} is the elastic modulus of the steel screws (= 30×10^6 psi).

The joint member stiffness for the adapter-plate-to-array-plate screwed connections is simply expressed as the parallel sum of the component member stiffnesses:

$$\frac{1}{k_{joint}} = \frac{1}{k_{adapterplate}} + \frac{1}{k_{arrayplate}}, \quad (26)$$

$$\text{where } k_{adapterplate} = \frac{0.577 \pi d_{nom} E_{plates}}{\ln \left(\frac{(1.15 t_{adapterplate} + D_{flats} - d_{nom})(D_{flats} + d_{nom})}{(1.15 t_{adapterplate} + D_{flats} + d_{nom})(D_{flats} - d_{nom})} \right)} = 8.27 \times 10^7 \text{ lb/in.},$$

$$k_{array} = \frac{0.577 \pi d_{nom} E_{plates}}{\ln \left(\frac{(1.15 t_{array} + D_{flats} - d_{nom})(D_{flats} + d_{nom})}{(1.15 t_{array} + D_{flats} + d_{nom})(D_{flats} - d_{nom})} \right)} = 10.85 \times 10^7 \text{ lb/in.},$$

and where E_{plates} is the elastic modulus of the steel adapter and steel array plates ($= 30 \times 10^6$ psi), E_{screw} is the elastic modulus of the steel screws ($= 30 \times 10^6$ psi), and D_{flats} is the distance between opposite flats of the bolt head for structural hexagonal screws² ($= 2.0$ in.). This results in

$$k_{joint} = 4.69 \times 10^7 \text{ lb/in.}$$

Once bending moment M_x is applied to the adapter-plate-to-array-plate screwed joints, the screws and joint members (i.e., adapter plates and array plates) will deform. For example, screws subjected to tensile axial reactions will elongate, and the initial compression produced in the joint members near these tensile-loaded screws will relax. The increased deformation within screws having tensile axial reactions will decrease the deformations in the joint members.

The total axial force on the screws F_{screw_total} is computed using the screw and joint member stiffnesses (equation (27)):

$$F_{screw_total_i} = \frac{k_{screw} F_{dpi}}{k_{screw} + k_{joint}} + F_{preload}, \quad (27)$$

where i is the screw row number and F_{dpi} is the corresponding reaction force at screws in the i^{th} row. The total axial forces are listed in table 12.

Table 12. Total Screw Axial Forces

Screw Location	Total Screw Axial Force (lb)			
	Deadweight Load Case		Overturning Load Case	
	Configuration 1	Configuration 2	Configuration 1	Configuration 2
Row 1	7,826	7,862	6,643	6,391
Row 2	7,699	7,703	7,546	7,514
Row 3	7,515	7,475	8,851	9,135

Note: Bolded values indicate increased tension beyond preload due to tensile axial reactions.
Non-bolded values indicate relaxation from compressive axial reactions.

The total normal stresses σ_{total} , which are simply the sum of the axial stress due to F_{screw_total} and the screw bending stress due to the shear path eccentricity σ_{bend_ecc} , are given for each screw by row according to the following equations and are listed in table 13:

$$\begin{aligned}\sigma_{total_1} &= \frac{F_{screw_total_1}}{A_t} + \sigma_{bend_ecc} , \\ \sigma_{total_2} &= \frac{F_{screw_total_2}}{A_t} + \sigma_{bend_ecc} , \\ \sigma_{total_3} &= \frac{F_{screw_total_3}}{A_t} + \sigma_{bend_ecc} .\end{aligned}\tag{28}$$

Table 13. Total Screw Normal Stresses

Screw Location	Total Screw Axial Stress (psi)			
	Deadweight Load Case		Overturning Load Case	
	Configuration 1	Configuration 2	Configuration 1	Configuration 2
Row 1	13,479	14,880	10,476	11,059
Row 2	13,348	14,716	11,409	12,217
Row 3	13,158	14,480	12,755	13,890

The maximum principal stresses for the screws σ_{max_prin} are computed in accordance with equation (29) and are listed in table 14:

$$\sigma_{max_prin} = \frac{\sigma_{total}}{2} + \sqrt{\left(\frac{\sigma_{total}}{2}\right)^2 + \tau_{screw}^2} .\tag{29}$$

Table 14. Maximum Screw Principal Stresses

Screw Location	Maximum Screw Principal Stress (psi)			
	Deadweight Load Case		Overturning Load Case	
	Configuration 1	Configuration 2	Configuration 1	Configuration 2
Row 1	13,584	15,027	10,536	11,145
Row 2	13,453	14,865	11,464	12,296
Row 3	13,265	14,631	12,805	13,959

The yield stress for the screws σ_{y_screw} is 81.0 ksi. The safety factor on screw yielding (see table 15) is simply

$$SF_{yield_screw} = \frac{\sigma_{y_screw}}{\sigma_{max_prin}} .\tag{30}$$

Table 15. Safety Factors on Screw Principal Stresses

Screw Location	Safety Factors on Screw Principal Stress (psi)			
	Deadweight Load Case		Overturning Load Case	
	Configuration 1	Configuration 2	Configuration 1	Configuration 2
Row 1	6.0	5.4	7.7	7.3
Row 2	6.0	5.4	7.1	6.6
Row 3	6.1	5.5	6.3	5.8

Shear tear-out of the threads in the array plate screw holes also needs to be addressed. The averaged shear stress in the threads due to screw pull-out $\tau_{threads}$ is computed as

$$\tau_{threads} = \frac{F_{screw_total}}{\pi d_s L_{engage}}, \quad (31)$$

where d_s is the shear diameter of the screw (= 1.065 in.), and L_{engage} is the length of thread engagement (= $t_{arrayplate}$ = 1.00 in.).

The shear yield stress of the array plates σ_{sy_plate} is obtained via the Maximum Shear Stress Theory² as

$$\sigma_{sy_plate} = \frac{\sigma_{y_plate}}{2} = 18.0 \text{ ksi}, \quad (32)$$

where σ_{y_plate} is the tensile yield stress of the array plates (= 36.0 ksi). The resulting values of $\tau_{threads}$ along with the thread shear safety factors as obtained from equation (33)) are given in table 16:

$$SF_{threadshear} = \frac{\sigma_{sy_plate}}{\tau_{threads}}. \quad (33)$$

Table 16. Average Screw Thread Shear Stresses and Safety Factors

	Screw Location	Average Thread Shear Stress (psi)		Safety Factor on Thread Shear Stress	
		Configuration 1	Configuration 1	Configuration 1	Configuration 1
Deadweight Case	Row 1	2,339	2,350	7.7	7.7
	Row 2	2,301	2,302	7.8	7.8
	Row 3	2,246	2,234	8.0	8.1
Overturning Case	Row 1	1,985	1,910	9.1	9.4
	Row 2	2,255	2,246	8.0	8.0
	Row 3	2,645	2,730	6.8	6.6

The foregoing calculation of $\tau_{threads}$ assumes that all threads equally support the load, which can be grossly in error. In contrast, Shigley and Mischke² state that only the first three full threads are required to develop the full strength of a bolt. Therefore, it is generally recommended that safety factors of >2.0 be used. The safety factors given in table 16 easily meet this recommendation. If sufficient ductility is present in the array plates and yielding does occur in the plate threads, the peak thread shear stress will redistribute so that additional threads will share the load. Therefore, upon yielding, a more uniform thread shear stress distribution will result.

3. SUMMARY AND CONCLUSIONS

Safety factors for the current Seneca Lake configuration 1 and 2 acoustic array/test fixture assemblies were evaluated through a series of detailed stress analyses. Particular attention was given to the I-beam-to-adapter-plate welds, the standoff pipes, and the adapter-plate-to-array-plate screws.

The finite element method was used to efficiently assess the stress resultants at key connection regions in the form of moments and forces for two specific loading cases. A nominal 1-g deadweight (hanging) load case was representative of the operational loads, and an overturning load case was established to conservatively provide sufficient structural integrity should excessive handling events occur during transport. The stress resultants were subsequently used in closed-form methods, together with assumptions commonly required in strength-of-materials calculations, to establish states of stress in the welds and screws. While no guidance was available for treating the joint member compressive stiffness for a screwed connection involving a threaded hole, the present analysis treated the joint member stiffness in accordance with that for a bolted connection. This assumption may warrant further investigation that is beyond the scope of the present effort.

Safety factors for the I-beam-to-adapter-plate welds exceeded the requirement of 5.0 on the allowable weld strengths. However, it is recommended that all welds be examined to ensure proper quality by using appropriate non-destructive inspection methods such as X-ray, ultrasonics, dye-penetrant, magnetic particle, etc., prior to lifting.

Safety factors on bending of the standoff pipes did not meet the requirement of 5.0 on the pipe yield stress and, therefore, require further design consideration.

Safety factors on screw principal stresses exceeded the 5.0 requirement against screw yielding.

Finally, safety factors on averaged screw thread shear stresses exceeded the 5.0 requirement against the screw shear yield stress. Although the use of averaged thread shear stresses can be in gross error as previously discussed, these safety factors meet the general requirement of exceeding 2.0 as suggested by Shigley and Mischke.²

REFERENCES

1. *ABAQUS Version 6.4*, ABAQUS Inc., Pawtucket, RI.
2. J. E. Shigley and C. R. Mischke, *Mechanical Engineering Design*, 6th Edition, McGraw-Hill, New York, 2001.
3. "Specification for Structural Joints Using ASTM A 325 or A 490 Screws," ASTM A325-07a, American Society for Testing Metals, www.astm.org/Standards/A325.htm.
4. E. F. Bruhn, *Analysis and Design of Flight Vehicle Structures*, Tri-State Offset Company, 1973, p. D1.9.

INITIAL DISTRIBUTION LIST

Addressee	No. of Copies
Defense Technical Information Center	2
Center for Naval Analyses	1
EG&G Technical Services Inc. (Attn: Emilio Recine) 349B Mitchell Street, Groton, CT 06340	5